# Use of sulfate and water isotopes to improve water and chemical balance estimates for water seeping from tailings basins (focus on US Steel's Minntac Basin)

An MWRAP 2 Final Report

Megan Kelly, Michael Berndt, and Travis Bavin

August 28, 2014

Minnesota Department of Natural Resources
Division of Lands and Minerals
500 Lafayette Rd.
St. Paul, MN 55155

# TABLE OF CONTENTS

# 1. ABSTRACT

The Minnesota Department of Natural Resources performed a chemical and isotopic investigation of waters in and around the Minntac Tailings Basin during 2011-2012. The aim of this study was to assess multiple processes that can influence sulfate concentrations in basin seepage waters. Samples were analyzed for major cations and anions, the isotope composition of water ($\delta^{2}H_{H2O}$ and $\delta^{18}O_{H2O}$) and the isotopic composition of dissolved sulfate ($\delta^{34}S_{SO4}$ and $\delta^{18}O_{SO4}$). This report details the methods used to calculate the impact of dilution, oxidation of sulfide minerals, and bacterial sulfate reduction on sulfate concentrations measured at seeps, wells, and stream downgradient of the basin.

Several approaches were taken to estimate the downstream dilution of mine-impacted water. Bromide and chloride appear to be suitable for use as conservative tracers, with similarly decreasing concentration profiles moving away from the tailings basin. However, initial chloride and bromide concentrations in the basin have changed over time, potentially impacting the calculated dilution effect. An alternative method involves the identification of characteristic water isotope end members and the application of mass balance calculations to estimate dilution by fresh water sources. A percent dilution was assigned for each downstream location sampled based on the combined evidence from the chloride, bromide, and water isotope measurements.

Sulfate concentration at many of the downgradient locations were higher than expected based on the applied dilution effect. Furthermore, a positive shift in sulfate isotopes provides the first clear indication that sulfate reduction is impacting the seepage waters. We simultaneous solve sulfate isotopic mass balance and Rayleigh equations to determine the amount of sulfide oxidation and sulfate reduction occurring around the basin. We calculate that up to 600 mg/L of "extra" sulfate is present in waters surrounding the basin, demonstrating that the oxidation of sulfide minerals in tailings does impact the sulfate concentration of seepage into both the Sand and Dark River watersheds. Sulfate is also being reduced and subsequently precipitated in the form of iron sulfide minerals as water seeps through the subsurface, reducing total sulfate concentrations by up to ~30%. It is critical, then, to account for these processes in the development of a basin sulfate balance.

# 2. INTRODUCTION

The release of dissolved sulfate from minelands continues to be an issue of concern for the iron mining region of Minnesota, in part due to the potential link between sulfate reduction and production of methyl mercury (MeHg), a toxic form of mercury that bioaccumulates in the food chain. While recent research efforts suggest that most MeHg is produced in non-mining influenced wetlands, high sulfate inputs at some specific wetland environments may promote the production and transport of MeHg (Berndt and Bavin, 2009; 11). There is also ecological,

economic, and cultural concern over the impact of sulfate levels on Minnesota's wild rice production. Minnesota's legal $SO_4$ standard for wild rice producing waters, 10 mg/L, was adopted in response to studies showing that wild rice grew only in low sulfate waters (Moyle, 1956). The standard is currently being reviewed, along with a detailed study of the linkages between elevated sulfate concentrations and the growth cycle of wild rice. Results of those studies will dictate the levels that need to be achieved during the growing season in all waters classified as wild rice producing waters. Through mixing with non-contaminated recharge waters, high concentrations of solutes (such as sulfate) in seepage waters are naturally attenuated moving away from the source. Dilution alone is often sufficient to bring downstream waters into compliance. However, particularly when this is not the case, it is important to have an understanding of chemical and biological reactions that can occur along the transport path.

Stable isotope information complements the hydrogeochemical methods often used to develop mine water and chemical balances, ultimately giving us a better understanding of the environmental impacts of mining activities. Isotopes have the potential to deliver information that is otherwise unattainable, uncovering previously overlooked complexities. At the same time, certain isotopic applications may be more cost- and time-efficient, as more information can be ascertained with fewer, precise measurements. Hydrogen and oxygen isotopes of water ($\delta^{2}H_{H2O}$ and $\delta^{18}O_{H2O}$) are relevant in mineland studies as they act as a natural fingerprint for different water bodies, allowing us to identify sources, evaluate mixing relationships, and estimate the impact of evaporative loss. Isotopes of dissolved sulfate ($\delta^{34}S_{SO4}$ and $\delta^{18}O_{SO4}$) can be used to trace the origin of sulfate and assess subsequent cycling processes.

This report focuses on the Minntac taconite mine property and surrounding area. Our study of seeps, monitoring wells, and downstream waters suggests that new $SO_4$ is added to the adjacent watersheds via oxidation of sulfide minerals in tailings. In addition, we find that that a considerable amount of sulfate reduction occurs as seepage escapes from the tailings basin and travels downgradient through the subsurface, potentially offsetting a portion of the impact from sulfide oxidation. Careful examination of isotopic information helps constrain the influence of both processes on the sulfate balance at the Minntac mine.

# 3. BACKGROUND

## 3.1. Water Isotopes

Isotopes are atoms of a given element that differ in mass due to the presence of additional neutrons. A water molecule, for example, has a different mass depending on what isotopes of hydrogen and oxygen are present. Heavy and light isotopes preferentially fractionate into different phases or reservoirs during certain physical, chemical, and biological processes. As a consequence, small differences in the isotopic composition can be observed, providing information on processes that have impacted the phase of interest over time. The isotope fractionation factor, $\alpha$, describes the isotope ratios of the coexisting reactant and product phases.

The fractionation between the liquid phase and the vapor phase of water can be described by the following equation:

$$\alpha = [^{18}O/^{16}O]_L/[^{18}O/^{16}O]_V$$

Isotope fractionation typically results in very slight changes in the isotopic ratios, and thus, isotope values themselves are reported as delta (δ) values, in per mil (‰) units relative to a standard.

$$\delta^{18}O\ (‰) = [(^{18}O/^{16}O)_{sample}/(^{18}O/^{16}O)_{standard} - 1] \times 1000$$

The isotope separation factor,

$$\varepsilon = 1000\ (\alpha_{l\text{-}v}\text{-}1) \approx \delta_L - \delta_V$$

is a more convenient way to express isotope fractionation, as this value also approximates the difference in δ-values between the two phases. Comparable equations apply for $^{2}H/^{1}H$ as well.

Isotope fractionation of water isotopes occurs during phase changes and meteorological processes. Mass-related differences in vapor pressure influence the $\delta^{2}H$ and $\delta^{18}O$ values of precipitation during rainout, with the isotopic composition of precipitation related to that of the source vapor by the equilibrium fractionation factor. The isotope separation factor for hydrogen, $\varepsilon_H$, is approximately 8 times greater than that for oxygen, $\varepsilon_O$. Consequently, the isotopic composition of global precipitation falls on a well-defined line in $\delta^{2}H$ and $\delta^{18}O$ space referred to as the "global meteoric water line" (GMWL, see Figure 1) with a slope of ~8 (Craig, 1961). Latitude, elevation, seasonal conditions and air mass history can all affect where the $\delta^{2}H$ and $\delta^{18}O$ of precipitation plots along the GMWL.

Evaporation of surface waters also generates a fractionation effect, in part due to the mass-related differences in vapor pressure; heavy molecules with lower vapor pressure are less likely to enter the vapor phase during evaporation. Molecular diffusion and turbulent transport of evaporated moisture across the water/air interface impart an additional kinetic fractionation effect during evaporation. The result is an enrichment in the heavy isotopes of both hydrogen and oxygen relative to the original composition of the water body. The composition of lake and river water recharge is approximately equivalent to that of local mean annual precipitation (MAP), which has a $\delta^{18}O_{H2O}$ of approximately -10.7‰ in the iron mining region of Minnesota, estimated using the online isotopes in precipitation calculator (OIPC) website (Bowen, 2013; Bowen et al., 2005; Bowen and Revenaugh, 2003) . The progressive impact of evaporation pulls the isotopic values away from the initial composition along a trend called a local evaporation line (LEL, see Figure 1).

Examination of the differences in isotopic composition of $\delta^{2}H$ and $\delta^{18}O$ therefore allows us to trace the origin and evolution of various waters. By identifying isotopic end member compositions, we can use simple mass balance equations to evaluate mixing and dilution. A

combined isotopic and mass balance, along with site specific climate parameters, can also be used to estimate the amount of evaporative loss (Gibson et al., 1993), especially important in the development a water balance for mining operations.

## 3.2. Sulfate Isotopes

### 3.2.1. Sulfide Oxidation

$\delta^{34}S$ values of dissolved sulfate can provide information on source mineralogy, while the $\delta^{18}O$ can help clarify the oxidation pathway responsible for forming the sulfate. The MN DNR has measured the concentration and isotopic composition of dissolved sulfate in mine pits and discharges across the Mesabi Iron Range of NE Minnesota (see Figure 2 for data, Figure 3 for location map). Figure 2a shows the $\delta^{34}S_{SO4}$ values vs. concentration of dissolved sulfate for the mine pit and discharge waters (Berndt and Bavin, 2012; unpublished data). Most data points fall between about +4 and +12‰, similar to the range of $\delta^{34}S$ values associated with primary sulfides in the iron formation (Carrigan and Cameron, 1991; Johnston et al., 2006; Poulton et al., 2010; Theriault, 2011). There is little to no net fractionation of sulfur isotopes during the oxidation of sulfide minerals (Taylor et al., 1984; Toran 1986; Toran and Harris, 1989), and thus the overlap in values suggests that the origin of dissolved sulfate in the mine waters is likely the oxidation of primary sulfide minerals. Alternatively, the range may represent a bulk average resulting from the oxidation of both primary and secondary sulfides. Mine pits with low sulfate concentrations, however, have $\delta^{34}S$ values that fall outside of the primary sulfide range, spanning between about -7 and +5‰. This suggests that at these sites, which tend to be located towards the western side of the iron range, the mineral source for dissolved sulfate source is predominantly secondary sulfides with more negative $\delta^{34}S$ compositions.

The oxygen isotopic composition of sulfate produced by the oxidation of sulfide minerals is a more complicated story. The $\delta^{18}O$ of sulfate is influenced by the specific oxidation pathway and the associated equilibrium and/or kinetic fractionation effects. Though the overall process involves a number of intermediate steps, pyrite oxidation is commonly described by two end member reactions,

(1) $FeS_2 + 3½O_2 + H_2O \Rightarrow Fe^{2+} + 2SO_4^{2-} + 2H^+$
(2) $FeS_2 + 14Fe^{3+} + 8H_2O \Rightarrow 15Fe^{2+} + 2SO_4^{2-} + 16H^+$

In Reaction 1, dissolved molecular oxygen ($O_2$) is the oxidant, whereas in Reaction 2 the oxidizing agent is ferric ($Fe^{3+}$) iron. Reaction 2 is limited by the supply of $Fe^{3+}$, and can proceed only as the supply of $Fe^{3+}$ is replenished by the oxidation of $Fe^{2+}$. According to the above reactions, sulfate oxygen can either come from $O_2$, with a $\delta^{18}O$ of +23.5‰, or oxygen from the water molecule, which typically has a negative $\delta^{18}O$. Locally, the oxygen isotopic composition of mean annual precipitation is approximately -10‰. The large difference in potential source

$^{18}O/^{16}O$ composition should allow for a closer examination of the sulfide oxidation process responsible for producing the sulfate.

However, most studies show that regardless of the oxidizing agent, water-oxygen is the dominant source of oxygen in the product sulfate molecule, and that $O_2$ does not interact directly with the sulfur atom during oxidation of sulfide minerals (Moses et al., 1987; Rimstidt and Vaughn, 2003). Isotopic investigations generally support this interpretation, but suggest that under certain conditions, a significant portion of the sulfate-oxygen can come from the isotopically heavier $O_2$ molecule (Taylor et al., 1984; Van Stempvorrt and Krouse, 1994; Balci et al., 2007). The oxidation of sulfide to sulfate involves a series of electron transfers, producing sulfoxy anions of intermediate oxidation states along the way such as thiosulfate ($S_2O_3^{2-}$) and sulfite ($SO_3^{2-}$). Depending on environmental conditions, such as pH and $O_2$ and/or $Fe^{3+}$ availability, intermediate species may dissociate from the mineral surface and accumulate in solution prior to the final oxidation to sulfate (Moses et al, 1987; Kohl and Bao, 2011). Experimental results indicate that isotope effects associated with the final intermediate sulfoxy anion, sulfite ($SO_3^{2-}$), may largely be responsible for the final signature of product sulfate (Müller et al., 2013). If sulfite oxidation is rapid relative to the exchange of $SO_3^{2-}$-oxygen with water, then the $\delta^{18}O$ of sulfite (with either a water or $O_2$ source) will be at least partially preserved in the sulfate. Slower oxidation allows more time for the oxygen isotopic signature of sulfite to be reset by equilibrium exchange with water and the associated fractionation effect. Again, the rate and extent of oxygen exchange are controlled by a combination of environmental factors.

Oxygen isotope values of dissolved sulfate in Mesabi Range mine pit and discharge waters vary along a trend between -11 and +5‰, and the cause of this variability remains unclear. However, there appears to be a link between $\delta^{18}O_{SO4}$ and sulfate concentration, suggesting that different processes are involved in the oxidation of sulfide minerals at different sulfate concentrations (Figure 2b). The range in sulfate concentrations, as noted earlier, also appears to be spatially dependent. Dissolved sulfate in waters from central-eastern locations have relatively high sulfate concentrations along with more negative $\delta^{18}O_{SO4}$, which implies that the sulfate-oxygen is derived entirely from the water molecule ($\delta^{18}O_{H2O}$ ~-10‰) with little to no net fractionation effect. Sulfate concentrations are lower in mine waters towards the western end of the iron formation, and these waters typically exhibit more positive $\delta^{18}O_{SO4}$ values. These relatively heavy oxygen isotope compositions may suggest a reaction pathway where $O_2$-oxygen is also incorporated into the product sulfate and/or may implicate the aforementioned interplay between the rates of sulfite oxidation and sulfite-water isotope exchange in shaping the isotopic composition of sulfate during sulfide oxidation (Müller et al., 2013).

### 3.2.2. Sulfate Reduction

The $^{34}S/^{32}S$ ratio of dissolved sulfate can also be used to determine whether and the degree to which bacterial sulfate reduction has impacted the initial sulfate pool. In the presence of an

organic carbon source (represented here by $CH_2O$), certain strains of bacteria are capable of simultaneously oxidizing organic carbon and reducing sulfate to gain energy for growth, as depicted in the following general equation:

$$2(CH_2O) + SO_4^{2-} = 2(HCO_3^-) + H_2S$$

The sulfate is reduced to $S^{2-}$in the form of $HS^-$, $H_2S$, or where iron is present, may precipitate as a solid Fe-sulfide. Lighter isotopes often accumulate in the product pool during isotope fractionation because of mass dependent thermodynamic properties. Chemical bonds in lighter isotopes are easier to break than the bonds in molecules containing the heavier isotopes. Therefore, the lighter $^{32}SO_4$ is preferentially utilized by the bacteria during metabolism. The sulfide produced will have a $\delta^{34}S$ that is isotopically lighter than that the source sulfate.

The pertinent isotope fractionation factor describes the ratio of $^{34}S/^{32}S$ in the coexisting reactant ($SO_4$) and product ($H_2S$) phases:

$$\alpha = [^{34}S/^{32}S]_{SO4}/[^{34}S/^{32}S]_{H2S}$$

and the isotope fractionation effect, ε, is related to the fractionation factor by the following formula:

$$\varepsilon = 1000\ (\alpha_{SO4\text{-}H2S} - 1).$$

We assume that a Rayleigh distillation process applies for $\delta^{34}S_{SO4}$ during sulfate reduction. Implicit in the Rayleigh model is the requirement that the product ($S^{2-}$) is instantaneously removed from the system as Fe-sulfide or $H_2S$ gas, and permanently isolated from the source $SO_4^{2-}$ pool. As mentioned above, the product sulfide is enriched in $^{32}S$ compared to $^{34}S$, and thus the residual dissolved sulfate pool becomes progressively enriched in $^{34}S$ compared to $^{32}S$. The Rayleigh Equation, shown below, describes the partitioning of isotopes and the reactant reservoir progressively decreases in size.

$$R = R_0 f^{(\alpha-1)}$$

In this equation, "$R_0$" refers to the initial $^{34}S/^{32}S$ ratio of the sulfate pool and "f" refers to the fraction of the original sulfate remaining. As reduction proceeds, "f" decreases and the $SO_4$ becomes progressively more enriched in the heavier $^{34}S$ (and $^{18}O$). We can also convert the isotope ratios to express the Rayleigh equation in delta notation:

$$\delta^{34}S_{SO4} = (\delta^{34}S_{SO4,init} + 1000)\ f^{(\alpha-1)} - 1000$$

Detailed studies of microbial sulfate reduction using both laboratory cultures and environmental samples show that the associated fractionation effect can vary widely. Laboratory studies typically give a range between ~2 and +46‰, but under certain conditions a fractionation effect of up to +70‰ is possible (Canfield and Teske, 1996; Detmers et al., 2001; Sim et al., 2011a).

The degree of isotope fractionation is controlled by an inverse relationship with the rate of sulfate reduction (slower rates lead to higher fractionations). Sulfate reduction rates, in turn, are impacted by a variety of factors, including the make-up of the bacterial community, sulfate concentration, temperature, and the type of organic substrate or fuel (Bruchert et al., 2001; Canfield, 2001; Detmers et al., 2001; Kleikemper et al., 2004; Sim et al., 2011b). For the purposes of this study, we adopt a value of $\alpha = 0.983$ ($\varepsilon = 17‰$). Berndt and Bavin (2011) arrived at this value using data from nearby sites where "f" was available using alternate methods.

While the lighter isotopes of oxygen are also generally favored during bacterial sulfate reduction as well, the oxygen isotopic signature of residual sulfate is again more complicated to interpret. The isotopic signature of oxygen potentially involves the recycling of sulfur intermediates and oxygen isotopic exchange with water/atmospheric $O_2$. Studies are underway to examine the isotopic response to the sulfate reduction process in more detail, and are discussed elsewhere in more detail (Kelly and Berndt, 2014b). We concentrate mainly on the $\delta^{34}S$ of sulfate to examine sulfate reduction in the vicinity of the Minntac mine property.

# 4. METHODS

## 4.1. Site Description

This study focuses on the United States Steel corporation Minntac tailings basin site in Mountain Iron, Minnesota (Figure 3), located in the central portion of the Mesabi Iron Range just north of the Laurentian Divide. The basin holds tailings produced during the processing of ore and also stores water for reuse in the plant facility. The basin covers a total area of 7612 acres, with an open water area (including Cell 1 and Cell 2 pools) of 1234 acres. Most of the water stored in the Cell 1 and Cell 2 pools is cycled back to the plant for use in processing. A portion, however, seeps from the bottom of the basin and through the perimeter dike into the surrounding watersheds, namely the Sand River watershed to the east of the basin and the Dark River watershed to the west. The concentration of dissolved sulfate is elevated in the Tailings Basin pool waters, and thus the seepage water that discharges into the Sand and Dark River watersheds is elevated as well.

## 4.2. Sample Collection and Analysis

Samples were collected for aqueous chemistry and environmental isotopes ($^{2}H/^{1}H$ and $^{18}O/^{16}O$ of water, $^{34}S/^{32}S$ and $^{18}O/^{16}O$ of sulfate) from in and around the Minntac plant and tailings basin. In December 2011, samples included the Mountain Iron Pit Reservoir, a number of plant process waters (Scrubber, Blowdown, Thickener, Agglomerator Process Water, Fine Tails), Tailings Basin Cell 1 (return water), two seepage collection sites at the eastern toe of the basin, and downstream on the Sand River. One liter water samples were collected by hand or with a Teflon sampling cup. In the case of Fine Tailings, sample water was decanted of the top after the solids

were allowed to settle. A similar set of samples was collected in September 2012, with the addition of Tailings Basin Cell 2 water, two monitoring wells on the east side of the basin, and a downstream site on the Dark River, which drains the west side of the basin. We returned in late October of 2012 to sample an additional suite of 8 monitoring wells around the perimeter of the basin (see Figure 2). Prior to sampling, monitoring wells need to be purged to ensure that fresh water samples are obtained. Minntac personnel bailed each well the day before our sampling visits, and on the day of, several well volumes were purged by pumping water through Teflon tubing attached to a portable peristaltic pump. Well waters were passed through a flow-through YSI cell to measure field parameters including temperature, pH, dissolved oxygen (DO), and conductance. Sampling commenced once the parameters had stabilized.

Major cation and anion samples were filtered at the DNR lab in Hibbing, MN with 0.45 µm PES filters, or at the site using a 0.45 µm cartridge filter. Cation samples were preserved with ultra-pure nitric acid and shipped on ice along with the anion samples for analyses by the University of Minnesota – Geochemistry Laboratory (Minneapolis, M) for analysis by ICP –AES and ion-chromatography, respectively.

All water isotope samples collected in 2012 were filtered using a 0.45 µm PES membrane filter and stored unpreserved in 30 mL HDPE bottles until shipped to University of Waterloo Environmental Isotope Lab for analysis. Bottles were tightly sealed with limited headspace to minimize further evaporative loss. Samples obtained in 2011 were collected in 1L bottles for both water and sulfate isotope analysis. The 1L samples were filtered in the Hibbing laboratory using 0.7 µm glass fiber filters and sent to the University of Waterloo for analysis. Water isotope samples were analyzed using standard isotope ratio mass spectrometry methods. $^{18}O/^{16}O$ abundance was determined via gas equilibration and head space injection into an IsoPrime Continuous Flow Isotope Ratio Mass Spectrometer (CF-IRMS). $^{2}H/^{1}H$ was determined via chromium reduction on a EuroVector Elemental Analyzer coupled with an IsoPrime CF-IRMS. Internal laboratory standards are calibrated and tested against international standards from the International Atomic Energy Agency (IAEA), including Standard Light Antarctic Precipitation (SLAP), Greenland Ice Sheet Precipitation (GISP), and Vienna Standard Mean Ocean Water (VSMOW). $\delta^{18}O_{H2O}$ and $\delta^{2}H_{H2O}$ are reported in ‰ relative to the international standard Vienna Standard Mean Ocean Water (VSMOW), which approximates the composition of the global ocean. Sample replicates are run approximately every 8 samples. Analytical uncertainties are ±0.2‰ and ±0.8‰ for $\delta^{18}O$ and $\delta^{2}H$, respectively.

Approximately 250 mL to 1 L water was collected for S and O isotope analysis of $SO_4^{2-}$. Samples were filtered after collection at the Hibbing laboratory using 0.7 µm glass fiber filter paper. All samples collected in 2012 were prepared for analysis at the DNR Hibbing Lab. Sulfate was extracted as solid $BaSO_4$ using procedures modified from Carmody et al. (1998). Water samples were first filtered through a 0.45 µm PES membrane filters. The filtrate was acidified with 1M HCl to a pH of 3-4 and heated at 90°C for ~ one hour so that any carbonate present would be degassed as $CO_2$. Approximately 6 ml of 6% $H_2O_2$ was also added to each

sample prior to heating to oxidize and degas any dissolved organic matter. These measures reduce contamination of the $BaSO_4$ precipitate. After heating, ~5 ml of 20% $BaCl_2$ was added (in excess) and the samples were allowed to cool for several hours or overnight. The $BaSO_4$ precipitate was collected on pre-weighed 0.45 µm PES membrane filters, and was dried overnight at 90°C. Once dry, the $BaSO_4$ powder was weighed, scraped into glass vials, and stored until shipment to the University of Waterloo Environmental Isotope Laboratory in Ontario, CA for isotopic analysis. Prior to the 2012 sampling season, water samples were shipped to the University of Waterloo, where they were then prepared for analysis in a similar manner.

The University of Waterloo Environmental Isotope Laboratory analyzed each $BaSO_4$ sample for $\delta^{34}S_{SO4}$ and $\delta^{18}O_{SO4}$. Relative $^{34}S$ and $^{32}S$ abundances for the precipitates were determined using an Isochrom Continuous Flow Stable Isotope Ratio Mass Spectrometer (GV Instruments, Micromass, UK) coupled to a Costech Elemental Analyzer (CNSO 2010, UK). Relative $^{18}O$ and $^{16}O$ abundances for the precipitate were determined using a GVI Isoprime Mass Spectrometer coupled to a Hekatech High Temperature Furnace and a Euro Vector Elemental Analyzer. $\delta^{34}S_{SO4}$ values are reported in ‰ units against the primary reference scale of Vienna-Canyon Diablo Troilite meteorite (VCDT), with an analytical precision of 0.3‰. $\delta^{18}O_{SO4}$ is reported relative to VSMOW, with analytical precision of 0.5‰.

## 5. RESULTS

Geochemical and isotopic results for mine plant, basin, and well waters are summarized in Table 1. Two wells that are classified as background waters, Monitoring Well 9 located west of the basin in the Slow Creek watershed, and Monitoring Well 10 located to the east in the Sand River watershed, were sampled in October 2012. These background waters have low $SO_4^{2-}$ concentrations, 0.1 and 11 mg/L, respectively. $Cl^-$ and $Br^-$ concentrations measured at these wells are also quite low, 0.4 and 1.4 mg/L for $Cl^-$ and 0.01 and 0.02 mg/L for $Br^-$. In comparison, concentrations in Tailings Basin Cell 1 are much higher, with and average $SO_4^{2-}$ of 970.5 mg/L, $Cl^-$ of 159.3 mg/L, and $Br^-$ of 1.2 mg/L. With the exception of Line 3 scrubber blowdown water, other process waters have concentrations similar to the basin waters. Seeps, wells and downstream sites have concentrations falling in between the background wells and the basin/process water values.

Water isotope values range from approximately -10‰ to -4‰ for $\delta^{18}O_{H2O}$ and -75‰ to -50‰ for $\delta^{2}H_{H2O}$. Tailings basin waters are relatively enriched in the heavy isotopes as they have been subject to a larger degree of evaporation than precipitation or fresh groundwater recharge sources. The average $\delta^{18}O_{H2O}$ of Minntac's Tailings Basin Cell 1 is -4.9‰, compared to mean annual precipitation in the area, -10.7‰. The background wells are both more depleted in $^{18}O$, both plotting close to the GMWL itself with isotopic values that suggest they are recharged

mainly by warm season (May-Oct) precipitation. Seepage collection waters along with mine-impacted wells and downstream locations fall along the evaporative trend in between the evaporation-impacted basin water and the recharge water. Relative contributions of the two end members can be determined for each site using isotope mass balance calculations. Line 3 scrubber blowdown water is more enriched in the heavy isotopes than all other waters, with average $\delta^{18}O_{H2O}$ and $\delta^{2}H_{H2O}$ of +1.8‰ and -42.6‰, respectively

The $\delta^{34}S$ and $\delta^{18}O$ of dissolved sulfate also vary widely depending on the type of water and location. Monitoring Well 9, one of the background sites, has very low $SO_4^{2-}$ concentrations (<1 mg/L) which prohibited isotopic analysis of sulfate. The other background well, Monitoring Well 10, had a measured sulfate concentration of 11 mg/L and a $\delta^{34}S_{SO4}$ value of +7.1‰ and a $\delta^{18}O$ value of +11.1‰. The isotopic signature of the background well is similar to background sulfate measured elsewhere in the region. Plant waters cluster between +7‰ and +8.6‰, with average Tailing Basin Cell 1 water $\delta^{34}S_{SO4}$ and $\delta^{18}O_{SO4}$ of +8.3‰ and +0.1‰, respectively. Average Mountain Iron Pit $\delta^{34}S_{SO4}$ is +5.8‰ and average $\delta^{18}O_{SO4}$ is -6.8‰. Mine influenced wells, seeps, and downstream waters are characterized by more positive isotopic values, ranging between +10.7‰ and +24.1‰ for $\delta^{34}S_{SO4}$ and between -2.7‰ and +7.6‰. Increasingly positive $\delta^{34}S_{SO4}$ is generally accompanied by more positive $\delta^{18}O_{SO4}$ values.

# 6. DISCUSSION

## 6.1. Dilution

Solute concentrations downgradient of the Minntac tailings basin generally fall in between those in the tailings basin pool waters and those measured at background wells. Intermediate values suggest that as water flows away from the basin, seepage is mixing with precipitation and/or uncontaminated groundwater. Water and chemical balance models often rely solely upon hydrological parameters to estimate fresh water infiltration, many of which are hard to attain. Alternatively, we can measure the dilution of the contaminated waters using different geochemical techniques. Each method is associated with its own limitations, but the inclusion of geochemical information can lead to a more accurate representation of how the mine signal is diluted along its flow path.

Certain chemical species are considered non-reactive and are therefore often used as conservative tracers. Measured concentrations of the conservative chloride ($Cl^-$) and bromide ($Br^-$) ions, for example, can provide information on water movement and dilution. Concentrations of these species are considerably elevated in Minntac pool and process waters relative to nearby background waters, likely due to the grinding and addition of fluxstone (marine dolomite, limestone) during pellet production (Engesser, 2006). The concentration of $Cl^-$ and $Br^-$ in surface, seep, and well water samples can be compared to basin waters to calculate the effect of dilution during transport.

Chloride and bromide concentrations measured in the Minntac Tailings Basin and the surrounding seep, monitoring well, and downstream sites correlate well, as demonstrated in Figure 4. The strong correlation substantiates the conservative nature of the two dissolved constituents. As a result, there is a good agreement between $Cl^-$ and $Br^-$-based dilution estimates for the seep and well waters (Table 2), which range from about 5% to 47%. The $Cl^-$-based dilution estimates tend to be slightly higher, particularly at PZ12, though the magnitude of these differences would have only minor implications for subsequent interpretations

Chloride and bromide dilution estimates, however, are made with the assumption that the initial concentrations are equal to the average of tailings basin waters sampled in 2011 and 2012 by the MN DNR. If the residence time for the water is long, on the order of decades, this may not be accurate as concentrations of both species have increased over time since flux pellet production began in 1986. If we are able to determine the amount of dilution using alternative means, we can assess the initial concentration assumption. To these ends, we also calculated dilution using isotope mass balance techniques. Using the isotope-derived estimates, we can then calculate starting basin water $Cl^-$ concentrations for waters collected from each well, accounting for the fact that the chemical composition of basin return water has changed over time. A lower than present initial basin $Cl^-$ concentration would qualitatively indicates a longer residence time.

The Tailings Basin Cell 1 pool is impacted by long-term evaporation (~35%, see Figure 5; Kelly and Berndt, 2013a) and thus enriched in the heavy isotopes of both oxygen and hydrogen, in addition to having elevated concentrations of $SO_4^{2-}$, $Cl^-$, and $Br^-$, when compared to background waters (see Table 1). In this scenario, we consider Cell 1 to be the mine impacted end member, called End Member #1 (see Figure 5), with a $\delta^{18}O_{H2O}$ of -4.9‰ and a $\delta^{2}H_{H2O}$ of -53.8‰. There are two options for opposing end members, one being the average basin recharge, which is represented by the intersection of the LEL with the GMWL and labeled as End Member #2 (Figure 5). The $\delta^{18}O_{H2O}$ of End Member #2 is -11.7‰ and the $\delta^{2}H_{H2O}$ is -84.0‰, similar to local MAP. The seepage collection waters, Mountain Iron Pit, and Monitoring Well 8, appear to fall on a trend between End Member #1 (Cell 1) and End Member #2 (LEL Recharge). Alternatively, End Member #3, which represents the average isotopic composition of background wells 9 and 10, might be a more appropriate choice for a mixing line for a number of the well locations. The background water composition suggests that groundwater at the background wells is recharged mainly from warm season precipitation, with average $\delta^{18}O_{H2O}$ = -9.6‰ and $\delta^{2}H_{H2O}$ = -68.3‰. This would be the case if winter snowfall did not infiltrate into the groundwater. The majority of well waters fall on or near the trend between End Member #1 (Cell 1) and End Member #3 (Background Recharge). Seepage collection and Pit waters, on the other hand, fall on the LEL recharge trend because they collect winter precipitation and annual snow melt in addition to the precipitation that falls during the warmer months.

For each well, we apply a mass balance to calculate the relative contribution of the two source end members, indicating how much dilution of basin water by either recharge waters has occurred. The estimates using both isotope end member methods are listed in Table 2. If an

unsuitable recharge end member is used, the calculations may give a starting $Cl^-$ concentration that is unreasonably high. This is apparent, for example, when Background Recharge is used as an End Member for the seepage pump back calculations. By considering all of the evidence, we can rule out any anomalous results and determine which method(s) are likely the most accurate representations of true dilution at each particular sampling location. These carefully determined "best estimates" are emphasized in bold face in Table 2 and retained for use in additional calculations.

## 6.2. Oxidation and Reduction

Unlike chloride and bromide, sulfate cannot be considered a conservative species in this environment, as lower $SO_4^{2-}$ concentrations at downgradient locations are only partially a result of dilution. Dissolved sulfate concentrations can also be modified by the oxidation of sulfide minerals and bacterial sulfate reduction. When dilution is taken into account, it becomes apparent that in several of the well/seep waters, there is actually excess (i.e. newly oxidized) sulfate present. Separating and quantifying the relative impact of these processes may be possible with the combined use of the previously described dilution estimates, along with additional isotopic information. More accurate tailings basin sulfate balances can ultimately be developed with the addition of this information.

The presence of excess sulfate is demonstrated visually on a plot comparing the estimated $SO_4^{2-}$ concentration vs. measured $SO_4^{2-}$ concentration (Figure 6). Divergence above the 1:1 trend indicates that sulfate has been added to the system. The wells that plot below the 1:1 trend, including PZ5, PZ12, and Monitoring Well 3, are all located on the east side of the basin, where a seepage collection and return system has been fully operational since June 2011. Seepage collection waters collected at Pumps 1 and 2 have both gained a considerable supply of additional sulfate. This suggests that the seepage pumps are succeeding in intercepting a large proportion of the high-sulfate surface seepage before it reaches the downgradient sites.

Net oxidation, the difference between the observed sulfate concentration and that predicted using the appropriate dilution factor, may not represent the actual amount of new sulfate produced. The presence of $H_2S$, readily identified at low concentrations by its strong odor, is often used as an indicator that sulfate reduction is occurring in the waters. Sulfide concentrations for all monitoring wells were analyzed by the MN Dept. of Health, and results were all very low, close to detection limits. However, as shown in Figure 7, there is a clear trend towards more positive $\delta^{34}S_{SO4}$ and $\delta^{18}O_{SO4}$ values, which indicates that sulfate is also being reduced as the water moves through the subsurface and seeps out from the tailings basin area. Therefore, the low sulfide concentrations in the groundwater may suggest that while sulfate reduction does occur, there is sufficient $Fe^{2+}$ present so that any $S^{2-}$ produced is precipitated out as Fe-S minerals. At the same time, the bacterial sulfate reduction process consumes $SO_4^{2-}$, decreasing the concentration at the

downstream sites beyond what is expected from dilution alone. Net oxidation in this situation would tend towards underestimating the actual gross amount of sulfate being added to the waters.

A combination of the above processes can affect the sulfate balance in and around a tailings basin, as pictured in Figure 8. To review, these include (1) dilution as precipitation infiltrates and mixes with mine impacted seepage, (2) oxidation of sulfides in tailings dike around the basin, adding new $SO_4^{2-}$ to the balance, and (3) reduction of sulfate in the subsurface, removing a portion of the $SO_4^{2-}$ from the balance and trapping it as Fe-sulfide minerals. We can simultaneously solve for the relative contribution of these processes using the relevant isotopic mass balance and Rayleigh equations. Results of this exercise are shown in Table 3.

It is important to note that several assumptions are necessary when making these calculations. To begin, we assume that the addition of new sulfate occurs prior to the sulfate reduction. Second, we need to assign a $\delta^{34}S_{SO4}$ value for the new sulfate generated in the tailings basin. Previously reported $\delta^{34}S_{SO4}$ values for Minntac East and West Pit waters fall within the range of results from other mine pit waters in the central portion of the range (Figure 2), consistent with the derivation from the oxidation of primary sulfide minerals in the iron formation. We consider the average of this data, which is +7.7‰, to be the composition of "new" sulfate added to the system resulting from the oxidation of primary sulfide minerals in the tailings. Finally, we assume that the sulfur isotope fractionation effect during sulfate reduction is 17‰, as mentioned previously.

Our calculations show that the relative amounts of oxidation and reduction vary around the basin. Except for PZ5 and PZ12, which fall downgradient of the seepage collection and return system, a considerable amount of newly formed sulfate is present. The largest estimated amount of oxidation, other than the seepage waters, is calculated for Monitoring Well 8 on the southwest side of the basin at just under 600 mg/L of additional sulfate. Sulfate reduction estimates at the well sites surrounding the basin generally range between ~150-400 mg/L. This translates to a reduction of ~15-30% of the total sulfate pool, which includes both the "old" sulfate seeping from the basin cell waters and the "new" sulfate from the oxidation of sulfide minerals in tailings. Spatial variability in sulfate reduction around the basin may relate to a combination of factors, including sulfate concentration, seepage rate, quality and availability of organic matter, variability in bacterial community, etc. On the east side of the basin, it appears that on average about 1/3 of the total sulfate pool is reduced and precipitated out as sulfide minerals. This is a particularly timely and important realization, as groundwater measured at PZ12 is currently flagged as exceeding Minnesota's drinking water sulfate standard of 250 mg/L. Work is being carried out to determine how best to reduce sulfate concentrations at this site. It is clear from isotope results that dilution of the high-sulfate basin water is only partially responsible for the concentration of sulfate measured in groundwater surrounding the basin. It is critical that oxidation of sulfide minerals in tailings and sulfate reduction are also considered in model development.

We tested the sensitivity of our oxidation and reduction calculations for each well using ε = +10, +17, and +25‰. Estimates appear to be most sensitive to a decrease in the fractionation effect. When a smaller fractionation effect value is used, a larger percentage of the total sulfate pool needs to be reduced in order to produce the required change in isotopic composition. Calculated values for both new sulfate produced and sulfate lost to reduction are much larger than the original estimates, up to and additional ~400 mg/L for each. As we would expect, using a higher value for the fractionation effect instead yields lower oxidation and reduction estimates. The differences, however, are not so large that they are unrealistic or qualitatively change the interpretations. We consider the original 17‰ value to be a sound choice in this case, but a slightly higher value may also be appropriate.

## 7. SUMMARY AND FUTURE WORK

A chemical and isotopic investigation of the Minntac Tailings Basin has shown that natural dilution of the high solute waters, oxidation of sulfide minerals within the tailings dike, and bacterial sulfate reduction in the subsurface are all important factors controlling the concentration of sulfate in well waters surrounding the basin. The latter two processes are often unaccounted for, as it is difficult to attain quantifiable estimates without the aid of isotopic measurements. For the first time, we can assign values to each of the three processes for the seep and well sites studied here. Additional work, however, may improve the accuracy of our estimates. Berndt (2011) developed a "framework model" to describe the isotopic evolution of dissolved sulfate with progressive sulfate reduction in the St. Louis River Watershed, using similar assumptions applied here for the oxidation and reduction calculations. Ongoing efforts are in place to refine aspects of the framework, including the fractionation effect associated with sulfate reduction as well as the initial composition of mineland sulfate. At the Minntac site, we may be able to further address the initial composition assumption through a direct examination of sulfide $\delta^{34}S$ in Minntac tailings core samples. The Minntac Tailings Basin investigation would also benefit from seasonal water isotope sampling to determine variability over the course of a year and to better pinpoint dilution end members, improving both our dilution and oxidation calculations. Additional sampling downstream on both the Dark and Sand Rivers, including flow data, would expand our ability to determine average basin seepage accounting for the processes detailed in this report. While these measures would be valuable to the Minntac tailings basin investigation, we may also learn a great deal by expanding this work to other mining operations in the area. This would enable us to better characterize sulfate behavior in seepage waters from a diverse group of settings.

## 8. ACKNOWLEDGEMENTS

The work described in this report was funded by the Minnesota DNR's Iron Ore Cooperative Research and Environmental Cooperative Research programs. Benjamin Von Korff and Katherine Rasley of the MN DNR helped with sample processing. We would like express our thanks to Minntac for cooperating with this research effort, particularly Tom Moe who facilitated and assisted with sample collection.

## 9. REFERENCES

Balci, N., Shanks III, W. C., Mayer, B., and Mandernack, K. W., 2007. Oxygen and sulfur isotope systematics of sulfate produced by bacterial and abiotic oxidation of pyrite. Geochimica et Cosmochimica Acta 71, 3796-3811.

Bavin, T., and Berndt , M., (2013) A Geochemical Mass Balance Method for Estimated Water and Sulfate Balances at Mining Facilities. A MWRAP 1 Interim Report, Minnesota Department of Natural Resources

Berndt, M.E., 2011. An interpretive framework for $\delta^{34}S_{SO4}$ and $\delta^{18}O_{SO4}$ in water samples from the St. Louis River Basin, in: Resources, M.D.o.N. (Ed.), Minnesota Department of Natural Resources Memo, 6 pages,

Berndt, M.E., Bavin, T.K., 2011. Sulfur and Mercury Cycling in Five Wetlands and a Lake Receiving Sulfate from Taconite Mines in Northeastern Minnesota: A Report to Iron Ore Cooperative Research Program., in: Resources, M.D.o.N. (Ed.). Minnesota Department of Natural Resources, Division of Lands and Minerals, St. Paul, MN, p. 77.

Berndt, M.E., Bavin, T.K., 2012. On the cycling of sulfur and mercury in the St. Louis River watershed, Northeastern Minnesota. An Environmental and Natural Trust Fund Report, Minnesota Department of Natural Resources, St. Paul, MN, 91 pages.

Bowen, G. J., 2013. The Online Isotopes in Precipitation Calculator, version 2.2. http://www.waterisotopes.org.

Bowen G. J. and Revenaugh J., 2003. Interpolating the isotopic composition of modern meteoric precipitation. Water Resources Research 39(10), 1299, doi:10.129/2003WR002086. (for annual average values)

Bowen G. J., Wassenaar L. I. and Hobson K. A., 2005. Global application of stable hydrogen and oxygen isotopes to wildlife forensics. Oecologia 143, 337-348, doi:10.1007/s00442-004-1813-y. (for monthly average values)

Brüchert, V., Knoblauch, C., and Jorgensen, B. B., 2001. Controls on stable sulfur isotope fractionation during bacterial sulfate reduction in Arctic sediments. Geochimica et Cosmochimica Acta 65, 763-776.

Canfield, D. E., and Teske, A., 1996. Late Proterozoic rise in atmospheric oxygen concentration inferred from phylogenetic and sulphur-isotope studies. Nature 382, 127-132.

Canfield, D. E., 2001. Biogeochemistry of sulfur isotopes. In: Valley,J.W., Cole, D.R. (Eds.), Reviews in Mineralogy and Geochemistry, vol. 43. Mineralogical Society of America, Blacksburg, VA, p. 607–636.

Carmody, R. W., Plummer, L. N., Busenberg, E., Coplen, T. B., 1998. Methods for collection of dissolved sulfate and sulfide and analysis of their sulfur isotopic composition. U.S. Geological Survey Open-File Report 97-234.

Carrigan and Cameron, 1991. Petrological and stable isotope studies of carbonate and sulfide minerals from the Gunflint Formation, Ontario: evidence for the origin of early Proterozoic iron-formation. Precambrian Research 52, 347-380.

Chapelle, F. H., Bradley, P. M., Thomas, M. A., McMahon, P. B., 2009. Distinguishing iron-reducing from sulfate-reducing conditions. Ground Water 47, 300-305.

Clark, I., Fritz, P., 1997. Environmental isotopes in hydrogeology. CRC Press/Lewis Publishers, Boca Raton, FL, p. 328.

Craig, H., 1961. Isotopic variations in meteoric waters. Science 133, 1702-1703.

Detmers, J., Brüchert, V., Habicht, K. S., Kuever, J., 2001. Diversity of sulfur isotopes fractionations by sulfate-reducing prokaryotes. Applied and Environmental Microbiology 67(2), 888-894.

Engesser, J., 2006. Evaluation of Minnesota Taconite Wet Scrubbers at Minntac, Keewatin Taconite, Hibbing Taconite, and United Taconite. Minnesota Department of Natural Resources, St. Paul, MN, 15 pages.

Gibson, J. J., Edwards, T. W. D., Bursey, G. G., Prowse, T. D., 1993. Estimating Evaporation using stable isotopes: Quantitative results and sensitivity analysis for two catchments in northern Canada. Nordic Hydrology 24, 79-94.

Heitmann, T., Blodau, C., 2006. Oxidation and incorporation of hydrogen sulfide by dissolved organic matter. Chemical Geology 235, 12-20.

Johnson, N. W., and Zhu, X., 2012. Carbon and iron additions to stimulate in-pit sulfate reduction and removal. University of Minnesota Duluth Research Report. 35 pages.

Johnston, D.T., Poulton, S.W., Fralick, P.W., Wing, B.A., Canfield, D.E., Farquhar, J., 2006. Evolution of the oceanic sulfur cycle at the end of the Paleoproterozoic. Geochimica et Cosmochimica Acta 70, 5723-5739.

Kelly, M. J., and Berndt, M. E., 2013a. A Water Isotope-Based Evaporation Model for US Steel's Minntac Tailings Basin. Minnesota Department of Natural Resources Memo, 12 pages.

Kelly, M. J., and Berndt, M. E., 2013b. An updated isotopic analysis of sulfate cycling and mixing processes in the St. Louis River Watershed. Minnesota Department of Natural Resources Memo, 22 pages.

Kleikemper, J., Schroth, M.H., Bernasconi, S. M., Brunner, B., and Zeyer, J., 2004. Sulfur isotope fractionation during growth of sulfate-reducing bacteria on various carbon sources. Geochimica et Cosmochimica Acta 68, 4891-2904.

Kohl, Issaku, and Bao, Huiming, 2011. Triple-oxygen-isotope determination of molecular oxygen incorporation in sulfate produced during abiotic pyrite oxidation (pH=2-11). Geochimica et Cosmochimica Acta 75, 1785-1798.

Moses, C. O., Nordstrom, D. K., Herman, J. S., and Mills, A. L., 1987. Aqueous pyrite oxidation by dissolved oxygen and by ferric iron. Geochimica et Cosmochimica Acta 51, 1561-1571.

Moyle, J., 1956. Relationships between water chemistry of Minnesota surface waters and wildlife management. Journal of Wildlife Management 30, 303-320.

Müller, I. A., Brunner, B., and Coleman, M., 2013. Isotopic evidence of the pivotal role of sulfite oxidation in shaping the oxygen isotope signature of sulfate. Chemical Geology 351, 186-202.

Poulton, S.W., Fralick, P.W., Canfield, D.E., 2010. Spatial variability in oceanic redox structure 1.8 billion years ago. Nature Geoscience 3, 486-490.

Rimstidt, J. D., and Vaughan, D. J., 2003. Pyrite oxidation: A state-of-the-art assessment of the reaction mechanism. Geochimica et Cosmochimica Acta 67, 873-880.

Sim, M. S., Bosak, T., and Ono, S., 2011a. Large sulfur isotope fractionation does not require disproportionation. Science 333, 74-77.

Sim, M. S., Ono, S., Donovan, K., Templer, S. P., and Bosak, T., 2011b. Effect of electron donors on the fractionation of sulfur isotopes by a marine *Desulfovibrio* sp. Geochimica et Cosmochimica Acta 75, 4244-4259.

Taylor, B. E., Wheeler, M. C., Nordstrom, D. K. 1984. Isotope composition of sulphate in acid mine drainage as measure of bacterial oxidation. Nature 308, 538-541.

Theriault, S. A., Miller, J. D., Berndt, M. E., and Ripley, E. M., 2011. The mineralogy, spatial distribution, and isotope geochemistry of sulfide minerals in the Biwabik Iron Formation. Institute for Lake Superior Geology, Abstract.

Theriault, S.A., 2011. Mineralogy, Spatial Distribution, and Isotope Geochemistry of Sulfide Minerals in the Biwabik Iron Formation, Geology. University of Minnesota, 165 p.

Toran, L., and Harris, R. F., 1989. Interpretation of sulfur and oxygen isotopes in biological and abiological sulfide oxidation. Geochimica et Cosmochimica Acta 53, 2341-2348.

Van Stempvoort, D. R., and Krouse, H. R., 1994. Controls of $\delta^{18}O$ in sulfate. Review of experimental data and application to specific environments. American Chemical Society 446-480.

Wels, C., and Robertson, A.M., 2003. Conceptual model for estimating water recovery in tailings impoundments. Tailings and Mine Waste: Proceedings of the Ninth International Conference, Vail, CO. Colorado State University, January 27-30, 2002. 459-468.

**Table 1:**
Geochemical and isotopic results for Minntac Waters collected in 2011 and 2012.

| Site Description | Date Collected | $Cl^-$ (mg/L) | $Br^-$ (mg/L) | $SO_4^{2-}$ (mg/L) | $\delta^{18}O_{H2O}$ (‰VSMOW) | $\delta^{2}H_{H2O}$ (‰VSMOW) | $\delta^{34}S_{SO4}$ (‰VCDT) | $\delta^{18}O_{SO4}$ (‰VSMOW) |
|---|---|---|---|---|---|---|---|---|
| **Mountain. Iron Pit** | **12/7/2011** | 28.6 | 0.10 | 349 | -9.8 | -72.8 | 5.7 | -7.3 |
| **Scrubber Makeup Water** | | 167.8 | 1.20 | 996 | -5.8 | -54.4 | 8.6 | -0.3 |
| **Line 5, Thickener Input** | | 207.6 | 1.32 | 1044 | -5.4 | -55.7 | 8.3 | 0.4 |
| **Lines 6 and 7, Thickener Input** | | 243.7 | 1.56 | 1110 | -5.1 | -55.2 | 7.9 | 0.3 |
| **Steps 1 and 2 Fine Tails** | | 181.2 | 1.28 | 1008 | -5.5 | -55.7 | 7.8 | -0.3 |
| **Step 3 Fine Tails** | | 191.2 | 1.38 | 1021 | -5.3 | -54.9 | 7.8 | 0.1 |
| **Line 3 Blowdown** | | 859.1 | 4.59 | 2446 | 2.2 | -43.9 | 6.8 | 3.7 |
| **Tailings Basin Cell 1 Return Water** | | 169.6 | 1.21 | 1008 | -5.0 | -56.4 | 8.4 | 0.0 |
| **East Seep; Pump 2; Catch Basin 10** | | 104.2 | 0.74 | 1006 | -7.1 | -64.9 | 10.9 | -0.9 |
| **East Seep; Pump 1; Catch Basin 5** | | 135.6 | 0.95 | 950 | -6.1 | -61.6 | 10.6 | 0.8 |
| **Sand River at Hwy 53** | | 43.8 | 0.24 | 212 | -8.2 | -68.2 | 17.6 | 7.6 |
| | | | | | | | | |
| **Mountain. Iron Pit** | **9/12/2012** | 28.0 | 0.11 | 312 | -9.5 | -74.7 | 5.9 | -6.2 |
| **Scrubber Makeup Water** | | 138.2 | 1.03 | 868 | -5.2 | -53.4 | 7.6 | 0.2 |
| **Lines 4 and 5, Thickener Input** | | 165.7 | 1.19 | 936 | -4.5 | -51.4 | 7.7 | 0.5 |
| **Lines 6 and 7, Thickener Input** | | 170.1 | 1.25 | 1058 | -4.3 | -52.5 | 7.2 | 0.6 |
| **Steps 1, 2, and 3 Fine Tails** | | 171.8 | 1.32 | 893 | -5.0 | -53.0 | 7.8 | -0.3 |
| **Step 2 Agglomerator Process Water** | | 171.5 | 1.30 | 1030 | -4.6 | -52.2 | 7.0 | 0.9 |
| **Step 1 Agglomerator Process Water** | | 165.7 | 1.23 | 946 | -4.7 | -51.9 | 7.2 | 0.3 |
| **Line 3 Blowdown** | | 842.0 | 4.89 | 2303 | 1.5 | -41.3 | 6.2 | 3.3 |
| **Tailings Basin Cell 2** | | 142.1 | 1.08 | 914 | -4.8 | -50.0 | 7.9 | 0.4 |
| **Tailings Basin Cell 1 Return Water** | | 148.9 | 1.12 | 933 | -4.8 | -51.2 | 8.2 | 0.2 |
| **East Seep; Pump 2; Catch Basin 10** | | 88.4 | 0.68 | 1121 | -8.0 | -68.4 | 12.2 | -2.7 |
| **East Seep; Pump 1; Catch Basin 5** | | 138.5 | 1.05 | 1031 | -6.5 | -62.1 | 10.7 | 0.5 |
| **PZ5** | | 147.8 | 1.14 | 742 | -5.4 | -54.8 | 14.4 | 5.8 |
| **PZ12** | | 101.1 | 0.83 | 479 | -6.2 | -58.4 | 15.2 | 5.6 |
| **Sand River at Hwy 53** | | 25.4 | 0.06 | 36 | -6.6 | -60.0 | 24.1 | 5.7 |
| **Dark River at CR 668** | | 85.7 | 0.60 | 710 | -6.1 | -55.2 | 13.0 | 3.5 |
| | | | | | | | | |
| **Well 3** | **10/25/2012** | 132.1 | 0.98 | 750 | -6.6 | -59.0 | 14.7 | 6.0 |
| **Well 4** | | 75.5 | 0.61 | 481 | -7.3 | -60.5 | 14.3 | 0.7 |
| **Well 6** | | 105.0 | 0.78 | 825 | -6.6 | -60.2 | 10.9 | -0.2 |
| **Well 7** | | 118.7 | 0.91 | 872 | -6.9 | -60.1 | 11.2 | 1.0 |
| **Well 8** | | 73.3 | 0.54 | 755 | -8.0 | -66.0 | 15.1 | 4.0 |
| **Well 9** | | 0.4 | 0.01 | 0 | -9.4 | -68.7 | | |
| **Well 10** | | 1.4 | 0.02 | 11 | -9.7 | -67.9 | 7.1 | 11.1 |
| **PZ12** | | 100.5 | 0.82 | 449 | -6.3 | -56.3 | 15.5 | 4.9 |

## Table 2:

All dilution estimates for seep and wells measured in 2011 and 2012. See text and Figure 5 for additional information regarding the isotope end members. The estimates that are used in the oxidation and reduction calculations are indicated in bold font.

| | | Dilution Estimate (%) | | | |
|---|---|---|---|---|---|
| **Site Description** | **Date Collected** | **Bromide** | **Chloride** | **Isotope – End Member #2** | **Isotope – End Member #3** |
| **E Seep Pump 2** | **12/7/2011** | 36.7 | 34.6 | **34.8** | 62.1 |
| **E Seep Pump 2** | **9/12/2012** | 41.9 | 44.5 | **47.1** | 83.7 |
| **E Seep Pump 1** | **12/7/2011** | 18.6 | 14.9 | **22.0** | 40.1 |
| **E Seep Pump 1** | **9/12/2012** | 9.4 | 13.0 | **25.5** | 45.8 |
| **PZ5** | **9/12/2012** | 2.1 | 7.2 | 5.1 | **8.4** |
| **PZ12** | **9/12/2012** | 28.8 | 36.6 | 17.2 | **29.8** |
| **PZ12** | **10/25/2012** | 29.8 | 36.9 | 14.7 | **23.9** |
| **Well 3** | **10/25/2012** | 15.7 | 17.1 | **20.9** | 35.7 |
| **Well 4** | **10/25/2012** | 47.4 | 52.6 | 28.9 | **49.0** |
| **Well 6** | **10/25/2012** | 32.6 | 34.1 | 23.1 | **40.2** |
| **Well 7** | **10/25/2012** | 21.5 | 25.5 | **25.2** | 43.3 |
| **Well 8** | **10/25/2012** | 54.0 | 54.0 | **43.2** | 75.5 |

**Table 3:**
Estimates for the fraction of sulfate added and fraction lost to reduction (in % and mg/L), using the best isotope-based dilution estimate (see text and Table 2).

| Site | Date Collected | Best Dilution Estimate (%) | New Sulfate (%) | Sulfate Reduced (%) | New Sulfate (mg/L) | Sulfate Reduced (mg/L) |
|---|---|---|---|---|---|---|
| **E Seep Pump 2** | **12/7/2011** | 34.8 | 46.8 | 15.5 | 557 | 184 |
| **E Seep Pump 2** | **9/12/2012** | 47.1 | 64.4 | 22.3 | 929 | 321 |
| **E Seep Pump 1** | **12/7/2011** | 22.0 | 31.2 | 13.6 | 343 | 150 |
| **E Seep Pump 1** | **9/12/2012** | 25.5 | 39.9 | 14.2 | 479 | 170 |
| **PZ5** | **9/12/2012** | 8.4 | 16.7 | 30.4 | 178 | 325 |
| **PZ12** | **9/12/2012** | 29.8 | 4.9 | 33.1 | 35 | 237 |
| **PZ12** | **10/25/2012** | 23.9 | -8.1 | 34.2 | -56 | 233 |
| **Well 3** | **10/25/2012** | 20.9 | 30.0 | 31.7 | 330 | 348 |
| **Well 4** | **10/25/2012** | 49.0 | 28.4 | 30.4 | 196 | 210 |
| **Well 6** | **10/25/2012** | 40.2 | 40.6 | 15.6 | 397 | 152 |
| **Well 7** | **10/25/2012** | 25.2 | 30.6 | 16.6 | 320 | 174 |
| **Well 8** | **10/25/2012** | 43.3 | 51.8 | 33.9 | 592 | 388 |

**Figure 1:**
General figure depicting trends in $\delta^{18}O_{H2O}$ and $\delta^{2}H_{H2O}$. The global meteoric water line (GMWL) is shown (Craig, 1961) along with the approximate distribution of summer vs. winter precipitation. The star represents the composition of mean annual precipitation (MAP). The local evaporation line (LEL) typically originates at that point, and proceeds along a line of shallower slope.

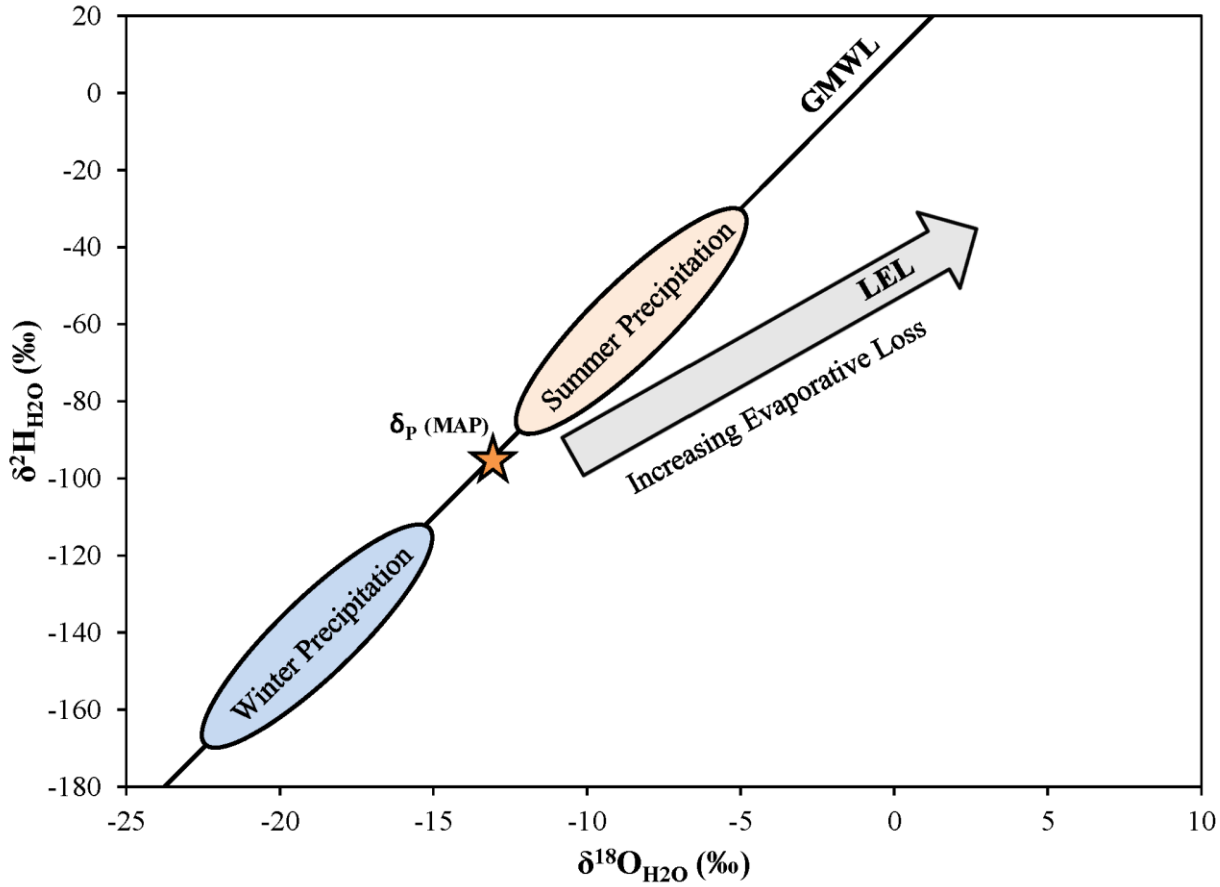

**Figure 2:**
Plot of (A) $\delta^{34}S_{SO4}$ vs. $SO_4$ concentration, and (B) $\delta^{18}O_{SO4}$ vs. $SO_4$ concentration for mine pit and discharge waters measured by the DNR over the last several years (Berndt and Bavin, 2012; unpublished data). Waters with sulfate concentrations ≤130 mg/L are from locations towards the western end of the Mesabi Iron Range (southwest of the Minntac Basin), and have isotopic compositions distinct from central-eastern locations.

**(A)**

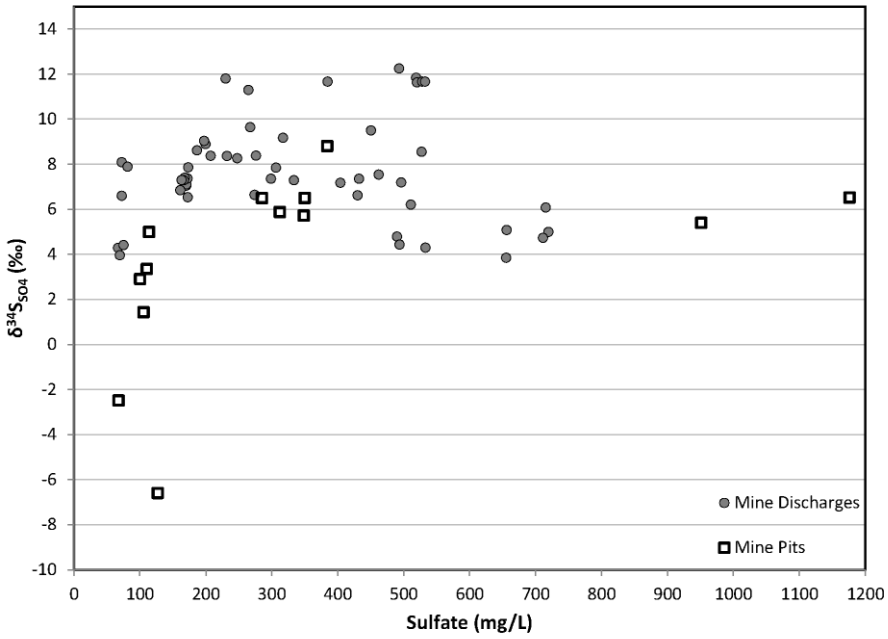


**(B)**

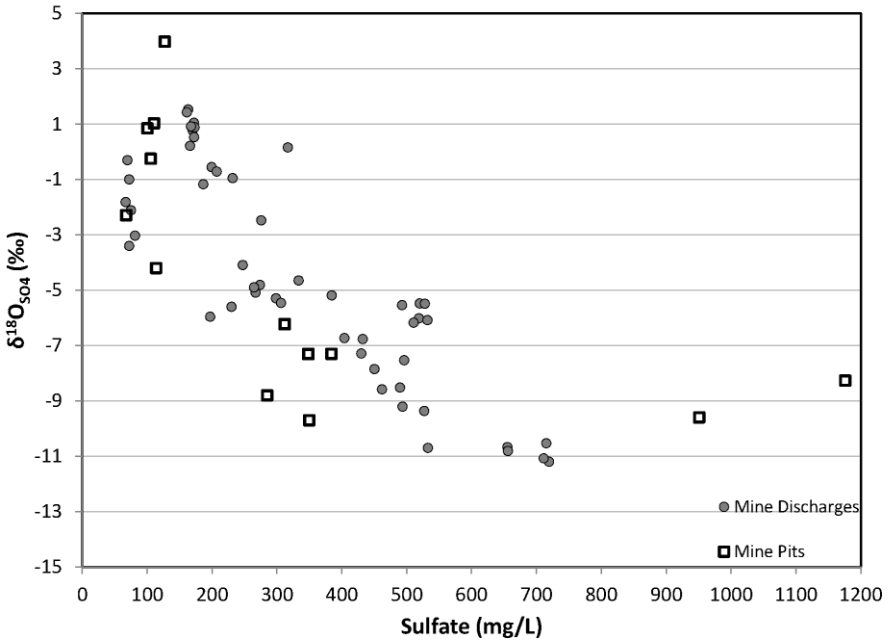

**Figure 3:**
(A) Map of Mesabi Iron Range in NE Minnesota, highlighting the location of taconite tailings basins and pits. The Minntac facilities are located in the central portion of the range. (B) Map of the Minntac Plant, Tailings Basin, and surrounding areas. The basin cell waters, seepage pumps, numbered wells, and stream sites are labeled.

**(A)**

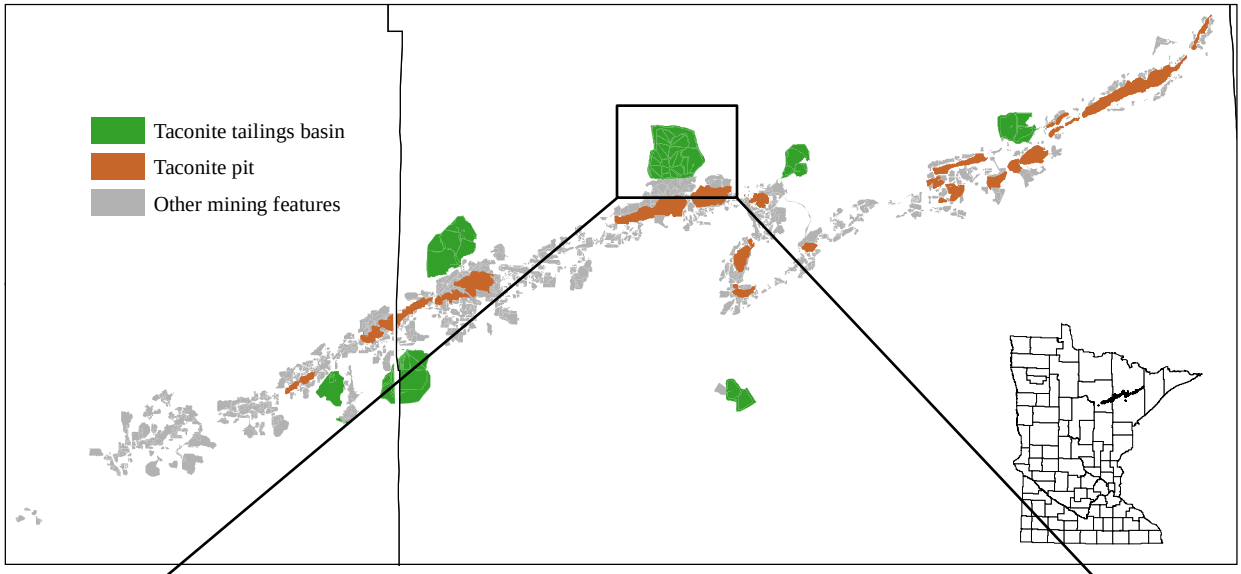


**(B)**

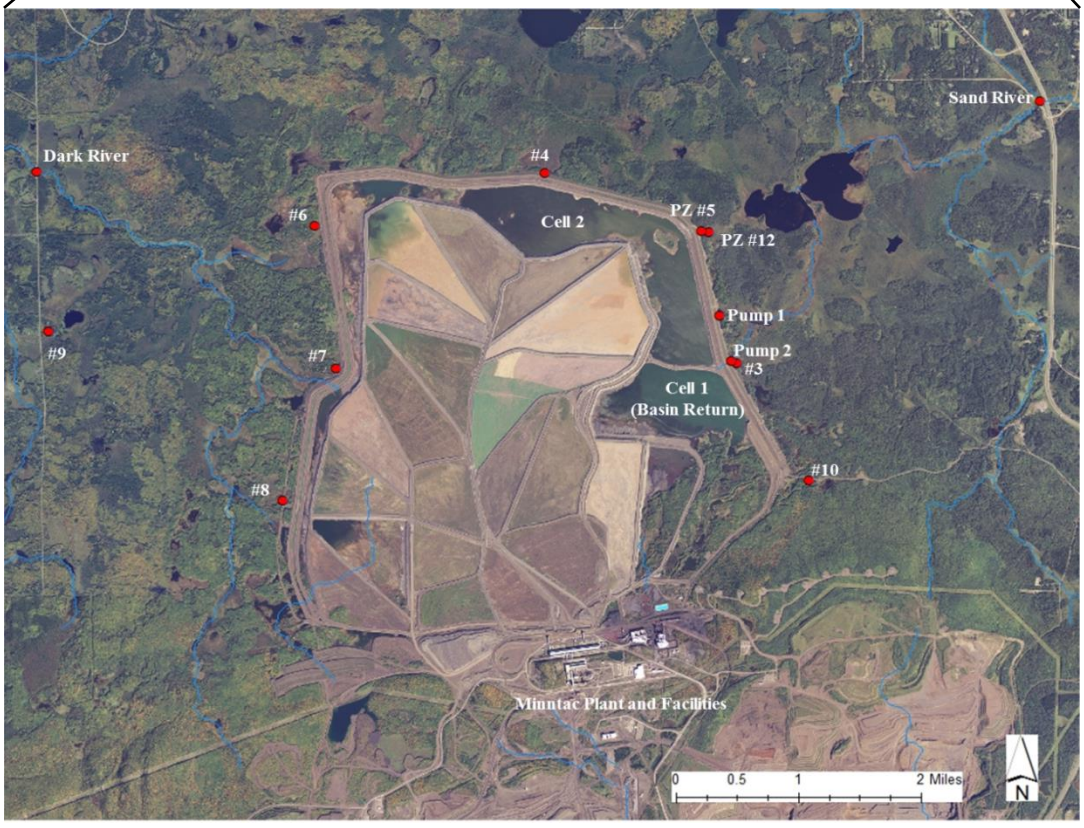

**Figure 4:**
Chloride vs. bromide concentrations measured in Minntac basin waters (black squares) and all downgradient locations, including seeps (brown circles), monitoring wells (blue triangles), and rivers (green triangles). Results are correlate well, with and linear regression $R^2$ value of 0.9732.

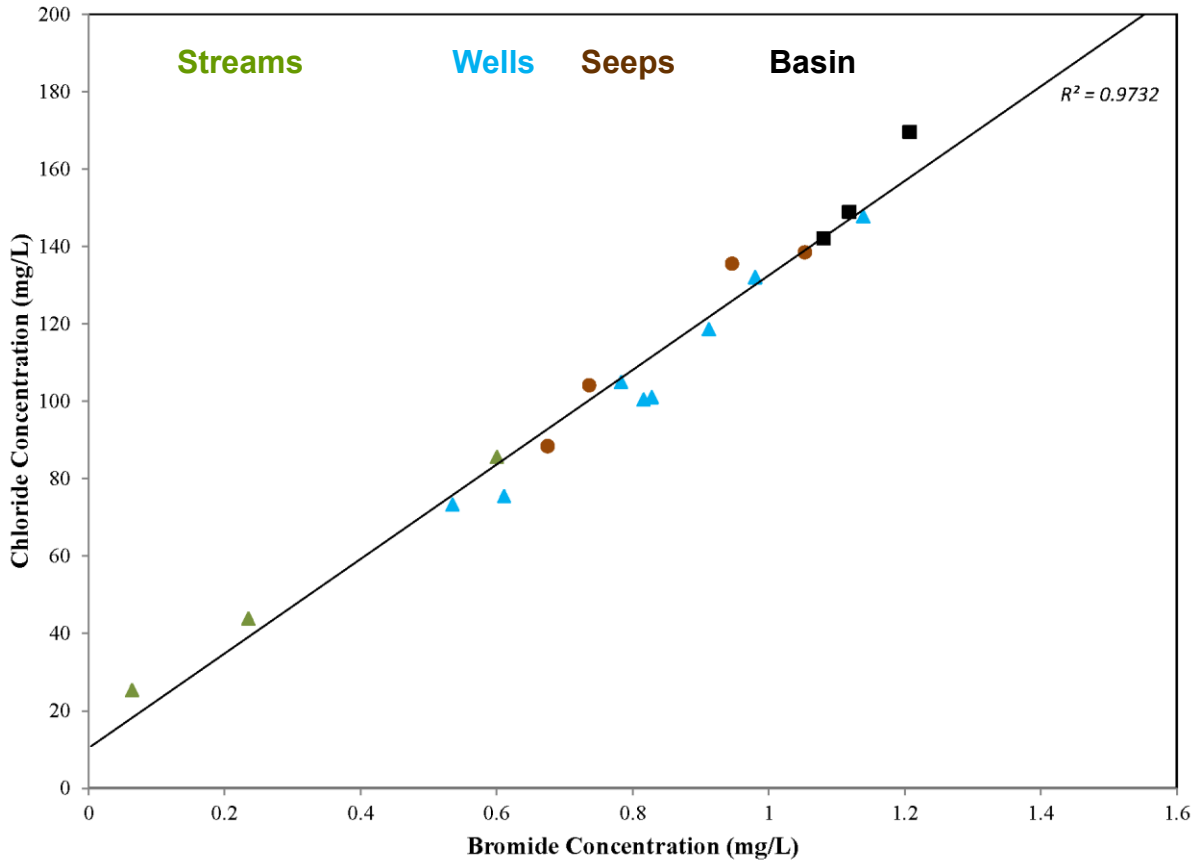

**Figure 5:**
**(A)** $\delta^2$H-$\delta^{18}$O plot showing data for Minntac Cell 1 Basin Return (black squares) and Mountain Iron Pit (black circles). Labeled star symbols represent the compositions of Global Meteoric Water Line (GMWL), Mean Annual Precipitation (MAP), mean May-October precipitation, and average recharge water. The modeled evaporative trend is shown (grey line), which indicates that ~35% of basin water is lost to evaporation.

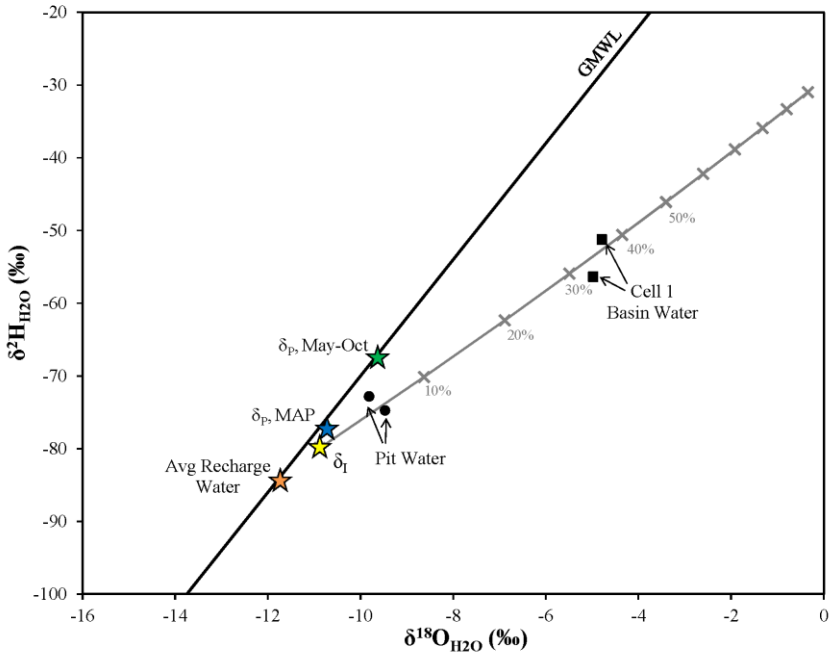


**(B)** Figure as above along with Minntac plant process waters (grey circles), seeps (brown circles), wells (blue triangles), and streams (green triangles). Two dilution trends between the different end members are also shown, as discussed in the text.

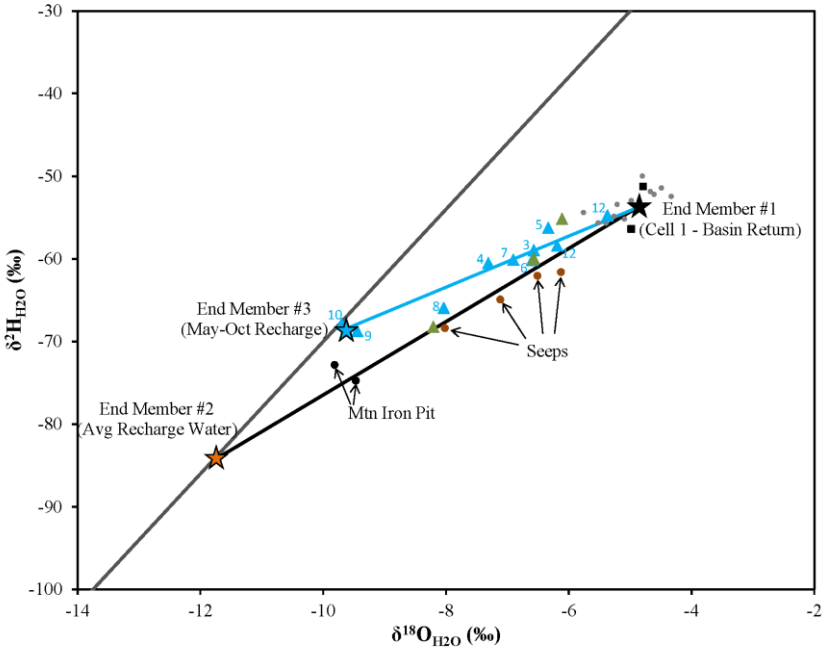

**Figure 6:**
Measured $SO_4$ concentrations for each well and seepage pump vs. those predicted based on dilution estimates. Data that falls above the 1:1 line indicate that more sulfate is present than expected if dilution alone were impacting the concentration.

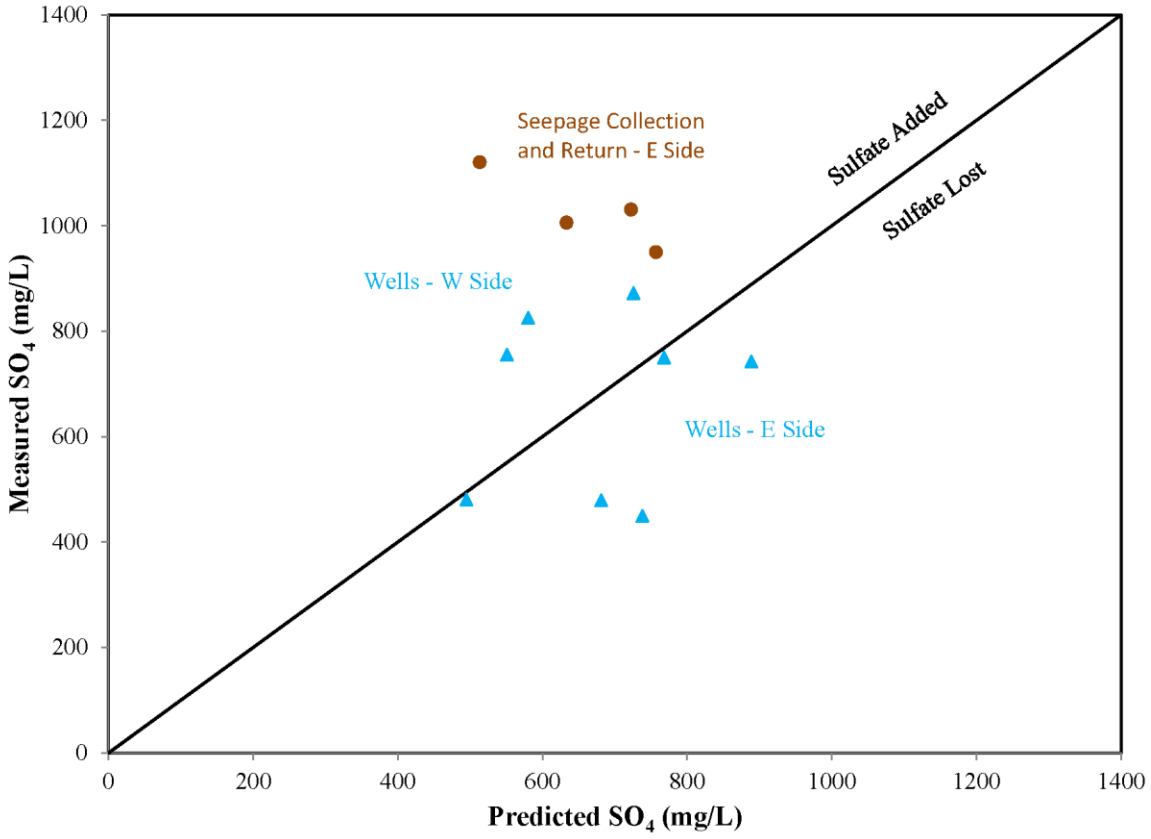

**Figure 7:**
Plot of $\delta^{18}O_{SO4}$ vs. $\delta^{34}S_{SO4}$for all samples from in and around the Minntac plant and basin, including Mountain Iron Pit (black circles), plant waters (grey circles), basin pool waters (Cell 1, black squares; Cell 2, orange square), seepage collection pumps (brown circles), monitoring wells (blue triangles), and stream waters (green triangles). The arrow depicts the increasing isotopic trend associated with bacterial sulfate reduction.

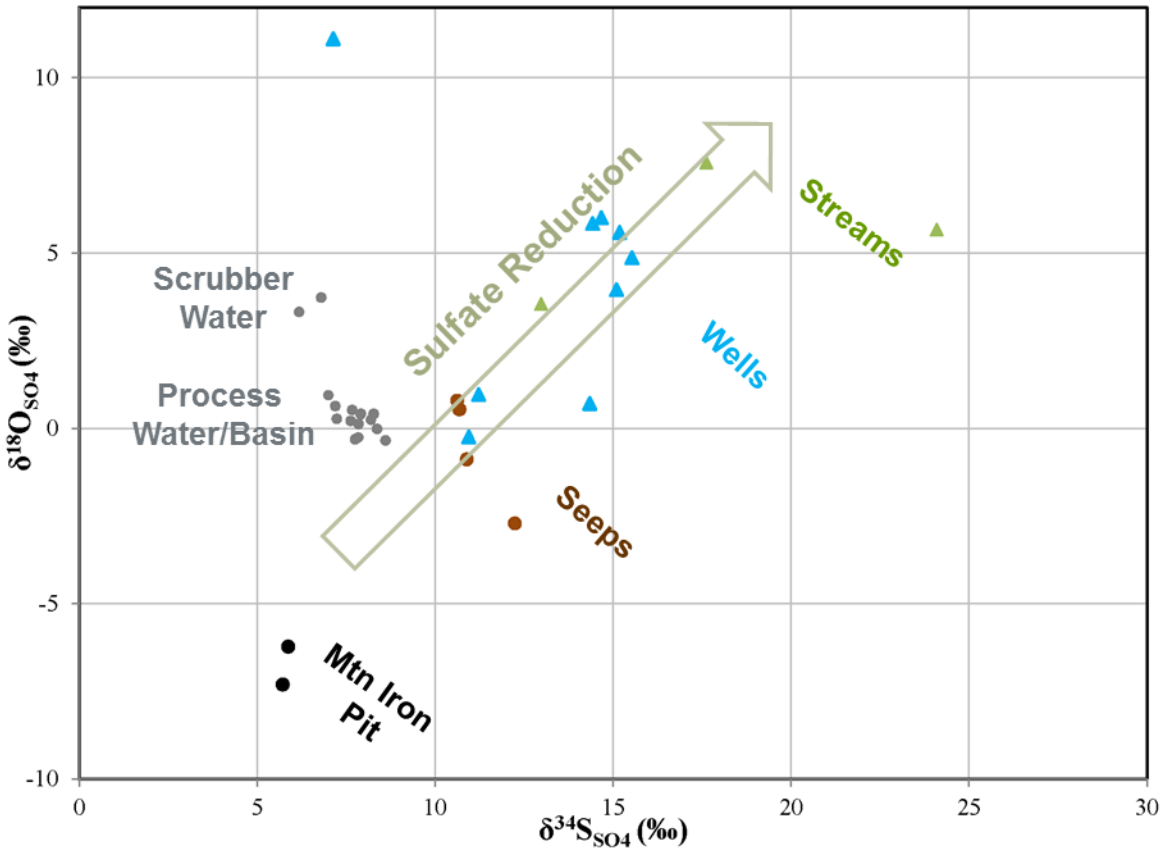

**Figure 8:**
Cross section view of a generalized tailings basin, including basin pool waters, tailings dike, and downgradient monitoring well (after Wels and Robertson, 2003). Processes that may impact the sulfate concentration and composition of waters surrounding a tailings basin are also shown, including dilution, sulfide oxidation, and sulfate reduction.